
17 Observation Payloads

17.1 Observation Payload Design

Jeffery J. Puschell, *Raytheon*

Observation payloads collect data (e.g., imagery, spectral radiance, distance) on remote objects such as the surface of the Earth, relatively nearby objects such as another satellite or distant astrophysical objects that can be processed into information (e.g., temperature, reflectance, chemical composition, topography) to provide insight into physical characteristics of these remote objects for scientific, weather forecasting, military and policy making purposes—just to name a few. Observation payloads operate across the entire electromagnetic spectrum from gamma rays and X-rays to RF frequencies. In addition, observation payloads include cosmic ray and other directional particle sensors used to probe the Sun, supernovae, active galactic nuclei and other unknown astrophysical objects. Table 17-1 lists the advantages of various observation payload types.

Two basic types of observation payloads exist: *passive payloads*, such as visible-infrared and microwave imagers that observe intrinsic emission from the scene, whether it be reflected sunlight, thermal emission or gamma rays. And *active payloads*, such as lidars and radars that supply their own source of light to enable specific types of measurement, such as ranging or to enhance signal-to-noise ratio and spatial resolution.

Space-based observation payloads include the following major categories.

Passive solar reflectance systems observe that part of the electromagnetic spectrum dominated by reflected sunlight—the ultraviolet ($\sim 0.3 \mu\text{m}$) through the short-wave infrared (SWIR) at $\sim 2.5 \mu\text{m}$. These systems offer the potential for relatively high spatial resolution from space, because their shorter operating wavelengths diffract less than longer wavelengths. However, because they rely on reflected sunlight for Earth observations, most of these systems operate effectively only during daytime. Observation payloads in this category include largely panchromatic imagers, like the GeoEye and DigitalGlobe commercial imagers, that specialize in collecting high spatial resolution imagery, multispectral (~ 10 spectral band with wavelength λ and spectral bandwidth $\delta\lambda$ such that $\lambda/\delta\lambda \sim 10$ typically), synoptic imagers like the GOES imager and polar orbiting environmental imagers like MODIS that provide routine global-scale observations (See Fig. 17web-1), hyperspectral (~ 100 spectral band with $\lambda/\delta\lambda \sim 100$ across a broad contiguous spectral region) imagers like Hyperion that provide more detailed spectral measurements over limited spatial regions, low light level imagers like the OLS onboard the DMSP satellite that provide panchromatic

imagery of moonlit or airglow lit scenes on Earth at night (Fig. 17web-2) and polarimeters such as POLDER that provide measurements of linear polarization of spectral radiance in different spectral bands across the entire solar reflectance spectral region.

Emissive or thermal infrared systems observe that part of the electromagnetic spectrum dominated by thermal emission from the scene itself in atmospheric transmission windows from $\sim 3 \mu\text{m}$ to $\sim 300 \mu\text{m}$ in wavelength. In some cases, these systems operate outside atmospheric transmission windows to enable less cluttered observations high above the surface of the Earth. These systems operate effectively day or night, because they do not rely on sunlight to create an observable signal. Like solar reflectance systems, emissive systems include multispectral imagers like the GOES imager (See Fig. 17web-3, Table 17web-1) and MODIS, hyperspectral systems like the Thermal Emission Spectrometer (TES) that flew on Mars Global Surveyor to map mineralogy on Mars and search for evidence of water (See Fig. 17web-4) and ultraspectral ($\sim 1,000$ spectral band with $\lambda/\delta\lambda \sim 1,000$ across a broad contiguous spectral region) systems like the AIRS sensor onboard the NASA Aqua satellite and the IASI onboard the Eumetsat MetOp satellite that provide detailed spectra of the Earth's atmosphere and surface to enable 3-D instantaneous maps of temperature distribution on the surface and in the atmosphere along with maps of water vapor and other trace gases.

Passive microwave systems observe thermal emission at much longer wavelengths than emissive infrared systems. The microwave part of the electromagnetic spectrum extends from $\sim 1 \text{ mm}$ to $\sim 1 \text{ m}$ in wavelength. Normally, microwave radiation is referenced to frequency rather than wavelength. In frequency, the microwave spectral region ranges from $\sim 0.3 \text{ GHz}$ to $\sim 300 \text{ GHz}$. Like emissive infrared systems, passive microwave systems operate effectively day or night. At frequencies less than 10 GHz , microwave radiation is relatively unaffected by clouds, so that these longer wavelength systems can operate under virtually all weather conditions. For higher frequency microwave systems, clouds and fog along with absorption by water and oxygen molecules in the atmosphere can influence the signal from the surface. Well known passive microwave systems include AMSU, SSM/I and SSMI/S (See Fig. 17web-5). AMSU is used primarily for mapping temperature and water vapor structure in the atmosphere. The system flying today is the most recent version of systems that have operated onboard the TIROS/POES satellites since 1978. SSM/I is used primarily for near-surface wind speed, total column water vapor, total column cloud liquid water and precipitation. It has been onboard DMSP satellites since 1987, but has



Fig. 17web-1. Spectacular True Color Image of the Hawaiian Islands Collected by the MODIS Onboard the Terra Spacecraft on 2003 May 23. The brighter surface area surrounding half of the islands is due to sunglint. Glint is not a desired feature in images used for ocean color studies, but does reveal turbulence in the surface waters of the Pacific Ocean. If the surface of the water was as smooth as a perfect mirror, we would see the circle of the Sun as a perfect reflection. But the surface of the water is roughened by waves and because each wave acts like a mirror, the Sun's reflection gets softened into a broader silver swath, called the sunglint region. (Photo courtesy of NASA)

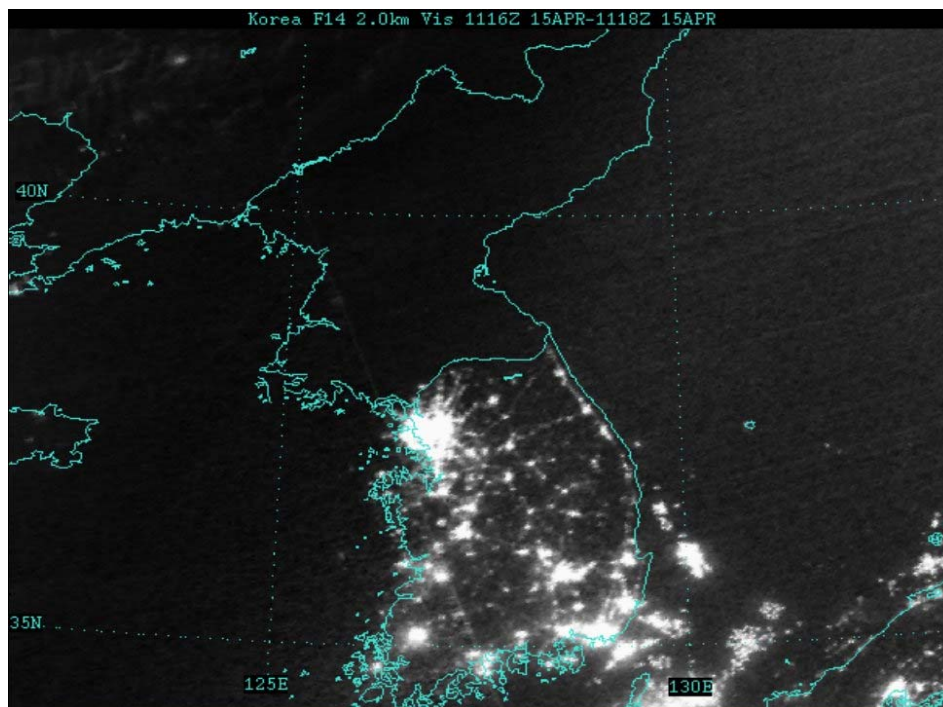


Fig. 17web-2. Low Light Level Imagery of the Korean Peninsula Collected by the OLS Onboard DMSP F14. (Photo courtesy of the US Department of Defense)

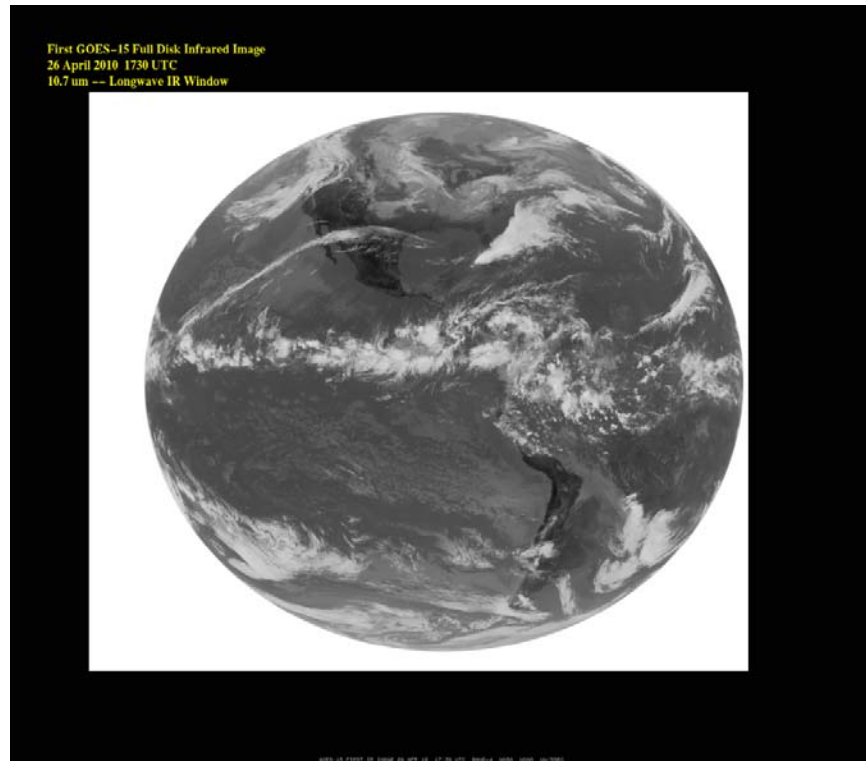


Fig. 17web-3. First Full Disk Emissive Infrared Image (10.7 μm band) from the Imager Onboard GOES-15. (Photo courtesy of NASA Goddard Space Flight Center, data from NOAA GOE.)

Table 17web-1. Summary of the Bands on the Current GOES Imagers from Hillger et al. (2003). The minimum and maximum wavelength range represent the full width at half maximum (FWHM or 50%) points.

Current GOES Imager Band	Approximate Wavelength Range (μm)	Central Wavelength (μm)	Nominal Subsatellite IGFOV (km)	Sample Use
1	0.53–0.75	0.65	1	Cloud cover and surface features during the day
2	3.8–4.0	3.9	4	Low cloud/fog and fire detection
3	6.5–7.0	6.7 (GOES-8/-11)	8	Upper-level water vapor
	5.8–7.3	6.5 (GOES-12+)	4	
4	10.2–11.2	10.7	4	Surface or cloud-top temperature
5	11.5–12.5	12.0 (GOES-8/-11)	4	Surface or cloud-top temperature and low-level water vapor
6	12.9–13.7	13.3 (GOES-12/-N)	8	CO ₂ band: Cloud detection
		13.3 (GOES-O/-P)	4	

heritage back to the Nimbus 7 and Seasat missions launched in 1978. SSM/I operates in seven channels ranging from 19 GHz to 89 GHz in frequency. AMSU is divided into two parts called A (used mostly for temperature sounding) and B (used mostly for water vapor sounding), which together operate in 20 spectral channels ranging from 23.8 GHz to 183.3 GHz in frequency and with different spectral resolutions for some frequencies. AMSU-A has a spatial sample size at nadir of about 45 km. The higher frequency AMSU-B has a spatial sample size of about 15 km at nadir. SSM/I operates with spatial resolutions ranging from 13 km to 69 km, depending on frequency. The SSM/I instrument is the

follow-on instrument to SSM/I and measures microwave energy at 24 discrete frequencies from 19 to 183 GHz with a swath width of 1,700 km at 12.5 km to 75 km spatial resolution at nadir. The synoptic solar reflectance and emissive infrared systems used in conjunction with these passive microwave systems operate with ~ 1 km spatial resolution using much smaller aperture sizes, because of the diffraction performance advantage of shorter wavelengths.

X-ray imagers observe thermal and non-thermal emission from astrophysical objects including the Sun, neutron stars, supernovae, the center of our Galaxy and distant unknown objects at wavelengths ranging from

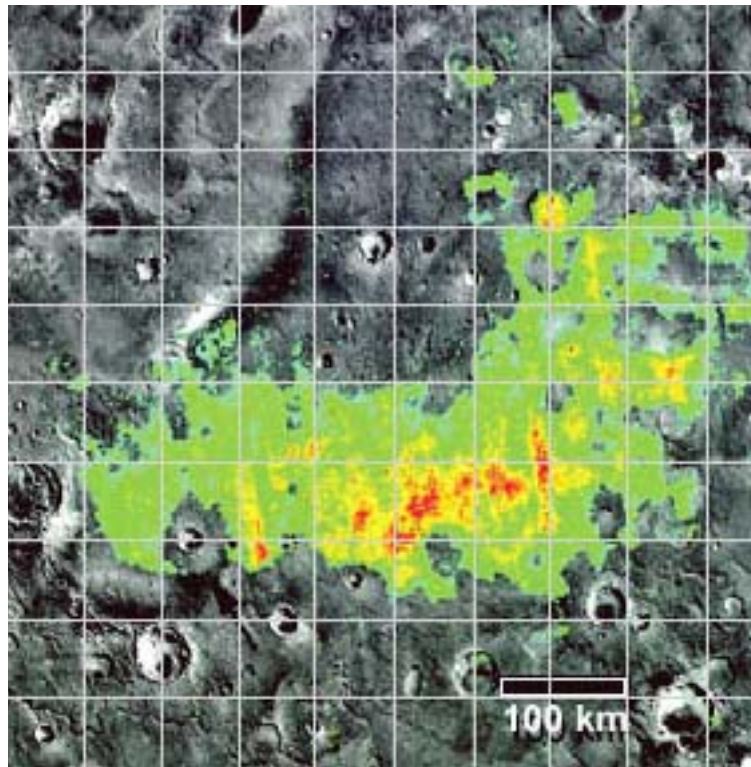


Fig. 17web-4. Analysis of Hyperspectral Data from the Infrared Spectrometer TES on-board Mars Global Surveyor Found Evidence for Past Surface Water on Mars by Mapping the Spectral Signature of Hematite, an Indicator of Dried-up Lakes. (Photo courtesy of Christensen et al.)

less than 3 pm to 10 nm, corresponding to frequencies ranging from above 10 EHz (1 EHz is 10^{18} Hz) down to 30 PHz (1 PHz is 10^{15} Hz). X-rays are often referenced in units of electron Volts (eV) rather than wavelength or frequency. In eV, the X-ray spectral region extends from about 0.1 KeV to 400 KeV. The first X-ray observations from space were made with Geiger counters that flew onboard converted V-2 rockets starting in 1949. UHURU also known as SAS-1 launched in 1970 was the first satellite with an X-ray observation payload. The Chandra X-ray observatory, launched in 1999, observes the 0.1 KeV to 10 KeV spectral region, with 2.4 μ rad (0.5 arcsec) angular resolution using a 1.2 m diameter X-ray telescope. The satellite is in a highly elliptical orbit that enables the observatory to make X-ray measurements (Fig. 17web-6) from well out the Earth's Van Allen belts. The effective collection area for the Chandra observatory is only 0.04 m² at 1 KeV, despite the much larger telescope diameter. Conventional optical approaches are not effective at X-ray wavelengths, because no suitable refractive material is available to build X-ray lenses and standard reflector telescopes do not work because X-rays are either absorbed or transmitted at near normal incidence to reflecting mirrors. Therefore, X-ray instruments use either a coded aperture method or a grazing incidence telescope also known as Wolter telescope to collect and focus X-rays. In Wolter telescopes, the angle of reflection from the mirror is

very low—typically 10 arcmin to 2 deg. Chandra uses a Wolter telescope that consists of nested cylindrical paraboloid and hyperboloid surfaces coated with iridium or gold. Chandra uses four pairs of nested mirrors. The relatively thick substrate (2 cm) and very careful polishing allowed a very precise optical surface, which is largely responsible for Chandra's unprecedented and unmatched angular resolution. However, thickness of the substrates limits the fill factor of the aperture, leading to the low effective collection area.

Gamma ray payloads observe emission of the highest energy photons from astrophysical objects including the Sun, supernovae, the center of our Galaxy and distant unknown objects. Gamma rays do not penetrate Earth's atmosphere very well so that direct astronomical observations of gamma rays must occur from high in the atmosphere or from space. Wavelengths for gamma rays are shorter than 3 pm, corresponding to frequencies greater than 10 EHz (1 EHz is 10^{18} Hz). The first gamma ray observations of the Sun and distant galactic and extragalactic objects were made by OSO-3 launched in 1967. Shortly thereafter, mysterious gamma ray bursts from very distant, but still only partially identified objects were discovered by the Vela satellites designed to detect gamma rays from nuclear explosions on Earth. Recent gamma ray observation payloads include the instruments onboard the Fermi Gamma Ray Telescope, a successor to the Compton Gamma Ray

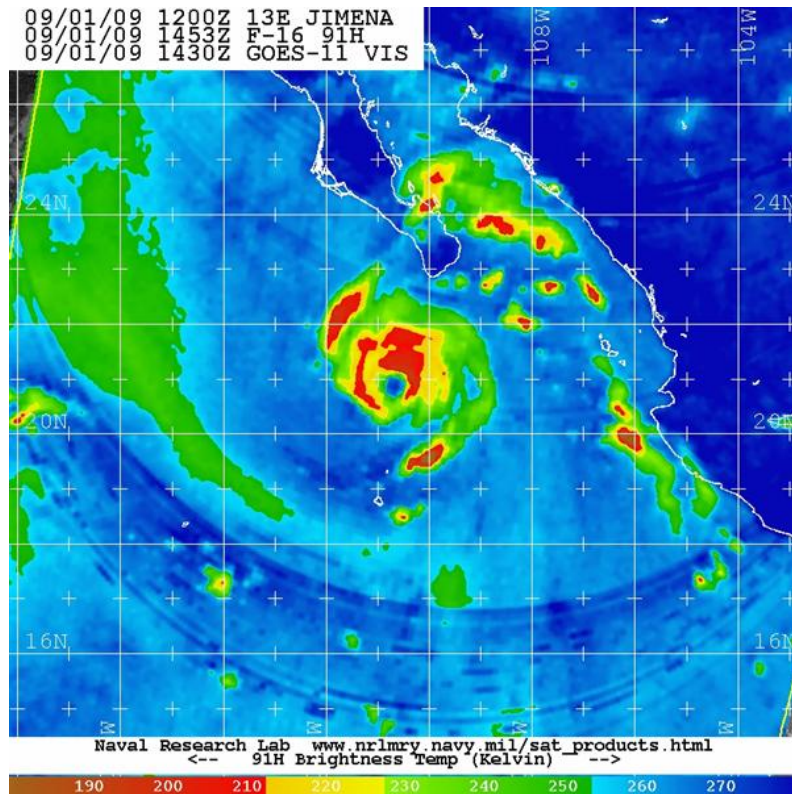


Fig. 17web-5. 91-GHz brightness Temperatures (in K) Measured by the SSM/I Passive Microwave Sensor on DMSP F-16, on 2009, September 1. The spiraling patterns of red, yellow, and green over and just south of Baja California indicate thunderstorms associated with Hurricane Jimena. (Photo courtesy of the US Air Force and the Naval Research Laboratory)



Fig. 17web-6. Chandra X-ray Observatory Image of the Region Near the Pulsar PSR B1509-58. This rapidly spinning neutron star, which was discovered by the Einstein X-ray observatory in 1982, is approximately 17,000 light years from Earth. The nebula surrounding the pulsar is about 150 light years in extent. In this image, the lowest energy X-rays that Chandra detects are red, the medium range is green, and the most energetic ones are colored blue. (Photo courtesy of NASA)

Observatory. These instruments detect gamma rays in two broad spectral ranges using scintillation detectors that detect small flashes of light created by gamma rays passing through a crystal and pair production techniques at the highest energies that create electron-positron pairs created by incoming gamma rays.

Active electro-optical systems like lidars, ladars and altimeters use active illumination of the scene by a laser to create a measurable signal that can be read out rapidly over time to remotely sense backscattered light from water droplets, aerosols and trace gases in the atmosphere as a function of distance from the system and for range measurements and altimetry, when looking at the Earth, Moon and other space objects. The first lidar in space was the Lidar In-space Technology Experiment (LITE) carried onboard the Space Shuttle in 1994. LITE measured clouds with a backscatter lidar based on a Nd:YAG laser operating at three different wavelengths: 1064 nm, 532 nm (second harmonic) and 355 nm (third harmonic). Figure 17web-7 illustrates the mission concept for LITE. CALIPSO, launched as part of the A-train of Earth Science satellites in 2006, is also a backscatter lidar based on a Nd:YAG laser. CALIPSO transmits both the fundamental (1064 nm) and second harmonic (532 nm) of the Nd:YAG laser in a nadir beam. The vertical resolution is 30 m and horizontal res-

olution 333 km. ICESAT launched in 2003 carried a Nd:YAG based laser altimeter used primarily for measuring thickness of Arctic ice sheets, but also for providing global topography and vegetation data. The main challenge for building a laser-based observational space payload is producing a reliable laser for extended duration use in space—previous instruments like ICESAT experienced failure of some laser modules after only a few months of operation. Lessons learned from ICESAT benefit future missions such as the upcoming AEOLUS mission with the ALADIN lidar, planned for the Atmospheric Dynamics Mission (ADM). ALADIN is a wind-measuring lidar, based on the third harmonic of a Nd:YAG laser. ALADIN will measure wind speed along the lidar line of sight by measuring the Doppler shift of the backscattered light using two methods: coherent (heterodyne) detection by mixing the return signal with a local oscillator and a direct direction method using a narrowband etalon. These techniques will be applied to measuring Doppler shifts of light returned to a receiver from Mie (aerosol) and Rayleigh (molecular) scattering respectively. While useful as a pathfinder for future winds lidar missions by providing information not available to today to numerical weather forecast models, AEOLUS will only measure a single component of the 3-D wind vector.

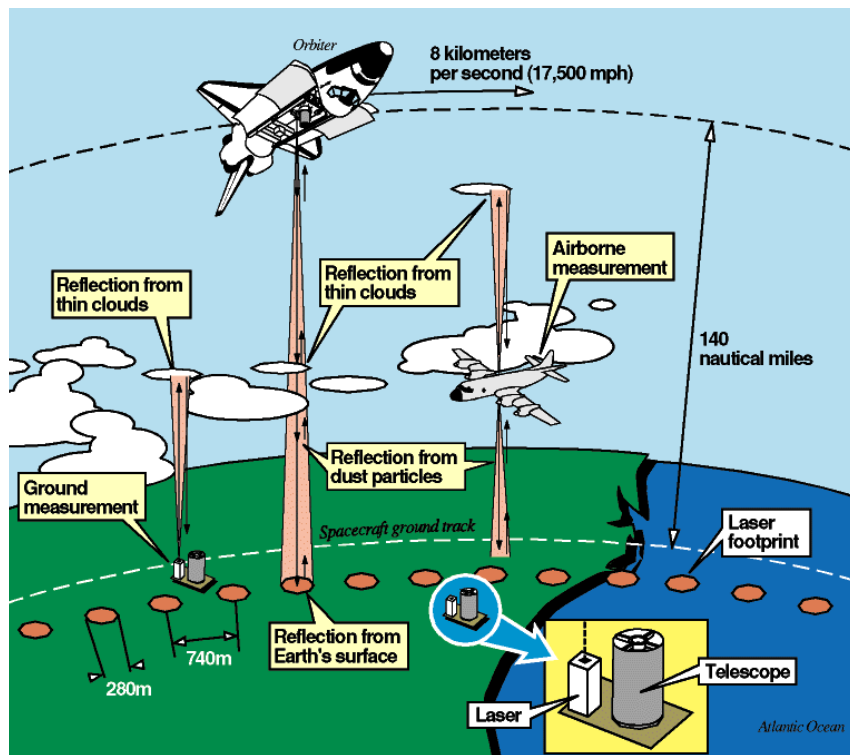


Fig. 17web-7. Mission Concept for the Shuttle Based LITE Lidar Experiment. Laser light from the Shuttle illuminates thin clouds, dust particles and the Earth's surface. Light reflected back to LITE's telescope is measured over with high temporal resolution to measure high and extent of clouds and particles above the Earth. Measurements from the ground and from aircraft provide ground truth information. (Photo courtesy of NASA)